Variability of horizontal temperature fluxes over the Arctic

D. Mewes, Ch. Jacobi

Institute for Meteorology, Stephanstr. 3, 04103 Leipzig,
E-Mail: daniel.mewes@uni-leipzig.de

Summary: We used ERA-Interim reanalysis data to perform a pattern analysis of the tropospheric mean meridional temperature flux in the Northern Hemisphere exploiting an artificial neural network called self organizing map (SOM). The basic explanation of the neural network will be given for a better understanding of the presented result. The neural network provides an analyses of the given data in terms of a decomposition into distinct patterns. The results confirms that the strongest fluxes occur over the North Atlantic. Additionally, the SOM showed that in general fluxes over the North Atlantic are most common over all analyzed winters.

Zusammenfassung: Wir verwendeten ERA-Interim Reanalysedaten. Dabei wurde für eine Analyse des über die Troposphäre gemittelten Temperaturflusses ein künstliches neuronales Netzwerks namens Selbstorganisierende Karte (Self Organizing Map, SOM) benutzt. Das neuronale Netzwerk hilft dabei den Datensatz in bestimmte Muster zu unterteilen. Die Ergebnisse bestätigen, dass die größten Flüsse über dem Nordatlantik in die Arktis vordringen. Weiterhin zeigt sich mithilfe der SOM-Methode, dass im Allgemeinen für den analysierten Zeitraum Flüsse über dem Nordatlantik häufiger sind als andere Pfade in Richtung Arktis.

1 Introduction

The Northern Hemisphere high latitudes are a very important region for the Earth's climate system, and acting as a net transmitter of radiation into space. Small changes in the properties of these regions will change the energy budget of the planet by changing the outgoing terrestrial radiation. With regard to climate change especially the Arctic has changed dramatically. During the last decades, the Arctic temperature is increasing approximately twice as fast as compared to the rest of the atmosphere (Stroeve et al., 2012). This effect is called "Arctic Amplification", and results from different feedback mechanisms in the Arctic (Wendisch et al., 2017), which enhance warming. The main positive feedback mechanisms are the surface albedo feedback, water vapor feedback, cloud feedback, and lapse-rate feedback, while the Planck feedback is negative (e.g. Colman, 2003; Klocke et al., 2013)

Another important aspect of Arctic Amplification is the decline of the meridional temperature gradient between the Tropics and the Arctic (Cohen et al., 2014), so that the general circulation is changing. Strong westerlies that are usual for the winter months are getting weaker and are resulting in more meandering winds. This itself results in more meridional

transport, where warmer air masses from lower latitudes are transported into the Arctic. This in turn leads leads to an increase of the temperature in Arctic regions and is further decreasing the meridional temperature gradient. To analyse Arctic Amplification, it is therefore necessary to quantify the meridional heat transport, and to elucidate its regional and temporal distribution.

To find distinct circulation patterns and to analyze the time variation of those patterns the artificial neural network Self Organizing Map (SOM) (Kohonen, 1998) can been used. SOMs are useful to find patterns within a given dataset, for example to find distinct pressure patterns. SOMs are becoming more and more used in the field of meteorology (Hewitson and Crane, 2002; Cassano et al., 2006; Lynch et al., 2016; McDonald et al., 2016; Ford and Schoof, 2017). The basic advantage of SOMs compared to other pattern analysis techniques (e.g. Principle Component Analysis (PCA), or empirical orthogonal Eigenfunction analysis, EOF) is that SOMs are not constraint to linear assumptions through the orthogonal decomposition of PCA/EOF. SOMs provides a decomposition that is closer to the data and sometimes easier to interpret physically, whereas PCA provides a mathematical orthogonal decomposition, which may sometimes be difficult to explain in physical terms.

The SOM method has been used to discover patterns of moisture transport over Greenland (Mattingly et al., 2016), which showed that from 2010-2015 compared to 1979-1994 intense water vapour transport to Greenland was more common. Furthermore, it was found that intense Greenland ice sheet melt seasons where preceded by moist winter conditions or occurred at summer times with record frequency of moist days. Cassano et al. (2016) analysed extreme temperature winter events for cold and warm days in Alaska. The synoptic conditions were extracted using the SOM method. They found that for either case temperature advection and anomaly in terrestrial downwelling radiation are the main contributors to the temperature extremes.

In the following we will analyse the large-scale meridional temperature flux in the high-latitude troposphere using the SOM-method. In section 2 the basic algorithm of the SOM neural network will be explained; in section 3 information about the used data will be provided. The results are presented in section 4 and discussed in section 5.

2 Self Organizing Map (SOM)

SOM is a neural network introduced by Kohonen (1998).This unsupervised learning method is able to reduce a high-dimensional input space into a two-dimensional map of nodes, which shows specific features of the given input vector $x(t)$. The created SOM consists of a two-dimensional array of patterns which are arranged in columns and rows. This neural network is based on an iterative process to train the map on a given input vector, which can be based on the formula

$$m_i(t + 1) = m_i(t) + \alpha(t)\, h_{ci}(t)\, [x(t) - m_i(t)]. \tag{1}$$

Here m_i is the current weight vector of node i, $\alpha(t)$ is the learning factor, and $h_{ci}(t)$ is a neighbourhood function, described by a Gaussian neighbourhood function,

$$h_{ci} = exp\left(-\frac{\| r_c - r_i \|^2}{2\, \sigma^2(t)}\right) \tag{2}$$

where r_c, r_i are the location vectors of node c and i. σ defines the width of the function and decreases over time.

At each iteration step each input vector is analysed by its Euclidean distance to each node and is then selected to the node according to the smallest distance. These closest input vectors are collected and are called best matching units (BMUs). Furthermore, each node is compared to their neighbours following h_{ci}, which describes the maximum radius of nodes c around node i to compare against. Then, according to $\alpha(t)$ the node changes to a new states. After these steps are performed for each node, the procedure is repeated until a predefined number of iterations has been performed. As a rule of thumb a SOM converges after a number of iterations that equals 50 times the number of nodes. Through the comparison of the node with its neighbours the map organizes itself in such a way that nodes that are close to each other are more similar compared to nodes that are father apart from each other. The amount of nodes within the map can be arbitrarily chosen. Choosing more nodes will provide more detailed patterns of the input data, whereas the training for only few notes is suitable to get a more generalized view of the input field.

In general, SOM are an alternative for a PCA or EOF analysis, but with the major advantage of a non-linear approach. Without linear assumptions SOMs can reproduce any pattern from a given dataset, which are dependant on non-linear interactions. Furthermore, the SOM method shows substantial advantages over PCA and (rotated) EOF analysis to find patterns in given data (Reusch et al., 2005; Liu and Weisberg, 2011).Reusch et al. (2005) found that SOMs, which are large enough, are more capable of extracting key features of a artificial generated dataset of pressure fields. Whereas PCA is less suitable to extract the predefined patterns, the SOM was able to reliably reproduce the predefined patterns in the artificial time series with correct attribution of variance. But it was also shown that the size of the SOM has to be big enough to extract the given patterns, and too small choices of SOM were not able to reproduce all patterns.

To create the SOMs, the python package "somoclu" was used (Wittek, 2013).The package is also available for R, MATLAB and for usage within the UNIX command line. Somoclu is computationally highly optimized to enable training of large maps and large datasets. As settings of the somoclu package we used 10000 iterations, $\alpha(t) = 0.5$ decreasing exponentially while iterating to 0.001. A SOM with 20 nodes was created with 4 rows and 5 columns. This means that 20 distinct patterns were produced which are aligned in a 2 dimensional grid of 5 patterns per row and 4 rows in total. The neighbouring maps/nodes starts to compare against a radius of 4 and the comparison was reduced exponentially during the iteration steps to just the closest neighbours. So the map learns/changes much during the very first iterations and then goes into the state of learning more specific from the given vectors.

It is important to look at the whole map and not just single nodes. This is necessary to get a view on how the algorithm has decomposed the field.

3 Data

For this study, synoptic (00, 06, 12, 18 UTC) ERA-Interim (Dee et al., 2011) winds and temperatures during the 1979 through 2016 winter seasons were used. The ERA-Interim data are available at a horizontal resolution of approximately 0.7 degrees, with 37 pressure levels from 1000 hPa up to 1 hPa. For the performed analysis the synoptic values were

daily averaged. For faster computation, the analysis was limited to regions north of 50°N. Daily data of Temperature T and meridional wind v where at first multiplied to obtained the meridional temperature flux in the unit of K m/s at each grid point. Afterwards the tropospheric mean from 1000 hPa to 200 hPa was calculated for each horizontal grid point:

$$F = \frac{1}{N} \sum_{i=p_0}^{p_1} (v_i(t, x, y) \, T_i(t, x, y)). \tag{3}$$

Here F is the final mean height, daily meridional temperature flux, p_0 is the lower pressure (200 hPa), p_1 is the higher pressure (1000 hPa), N is the number of pressure levels between p_0 and p_1, v_i and T_i are the meridional wind and temperature at a given pressure level i, and t, x, y represents time, meridional anad longitudinal dependcy. The unit of F is $\mathrm{K\,m\,s^{-1}}$, so large values for F represent a higher temperatures that are moved within a strong meridional wind. Lower values correspond to a weaker meridional transport or a lower temperature to begin with. The 2D-field of the mean height, mean daily meridional temperature flux F is then fed into the SOM algorithm.

4 Results

Figure 1 shows a 4x5 SOM after 10000 iterations as explained before. For easier comparison we denote each pattern corresponding to its position within the map with "node (j,k)". Here j denotes the row and k denotes the column according to the nomenclature for matrix indices. The contours show the tropospheric mean meridional temperature flux with the occurrence frequency during the analysed time period shown on the upper left corner. In general, there are three patterns which can be distinguished: one where the flux is strongest mostly over the Denmark Strait, one where flux is directed via the west coast of Greenland and another one where the flux is focused over the Bering Strait. Patterns that look similar to wedges of a pie near the pole are a result from the definition of the meridional wind which is only positive for northward wind. This results to such wedge shaped contours in polar projection maps.

Additionally, there are some patterns with an increased flux over the Laptev Sea (8 out of 20), or over the Kara Sea (3 out of 20). The strongest meridional temperature fluxes of $3600\,\mathrm{K\,m\,s^{-1}}$ occur only at about 5.5 % of the time (node (0,2)). The most frequent pattern occurs during 9.7 % of the analysed winters and favours fluxes over a North Atlantic pathway into the Arctic. The second most frequent pattern occurs during 9.4 % of the time and is mainly dominated by fluxes over the Bering Strait. Those major pathways were also found for moist static energy flux based on an analysis of 25 years of the Geophysical Fluid Dynamics Laboratory (GFDL) dataset (Overland et al., 1996). Other patterns are less frequent and only occur at about 2.4 % up to 3.1 % of the analysed time period. This may be a hint that the chosen size of the whole SOM is already too large to get a generalized view on the data, and might already show very specific patterns. Nevertheless, it can be seen that patterns that are close to each other are more similar compared to patterns that are farther apart. But it can also be seen that the difference between neighbouring patterns are not the same. For example, looking at the pattern in node (2,3), the right neighbour is *closer* to this node compared to the left neighbour. In further analysis these different distances have to be visualized in a way that one can easily
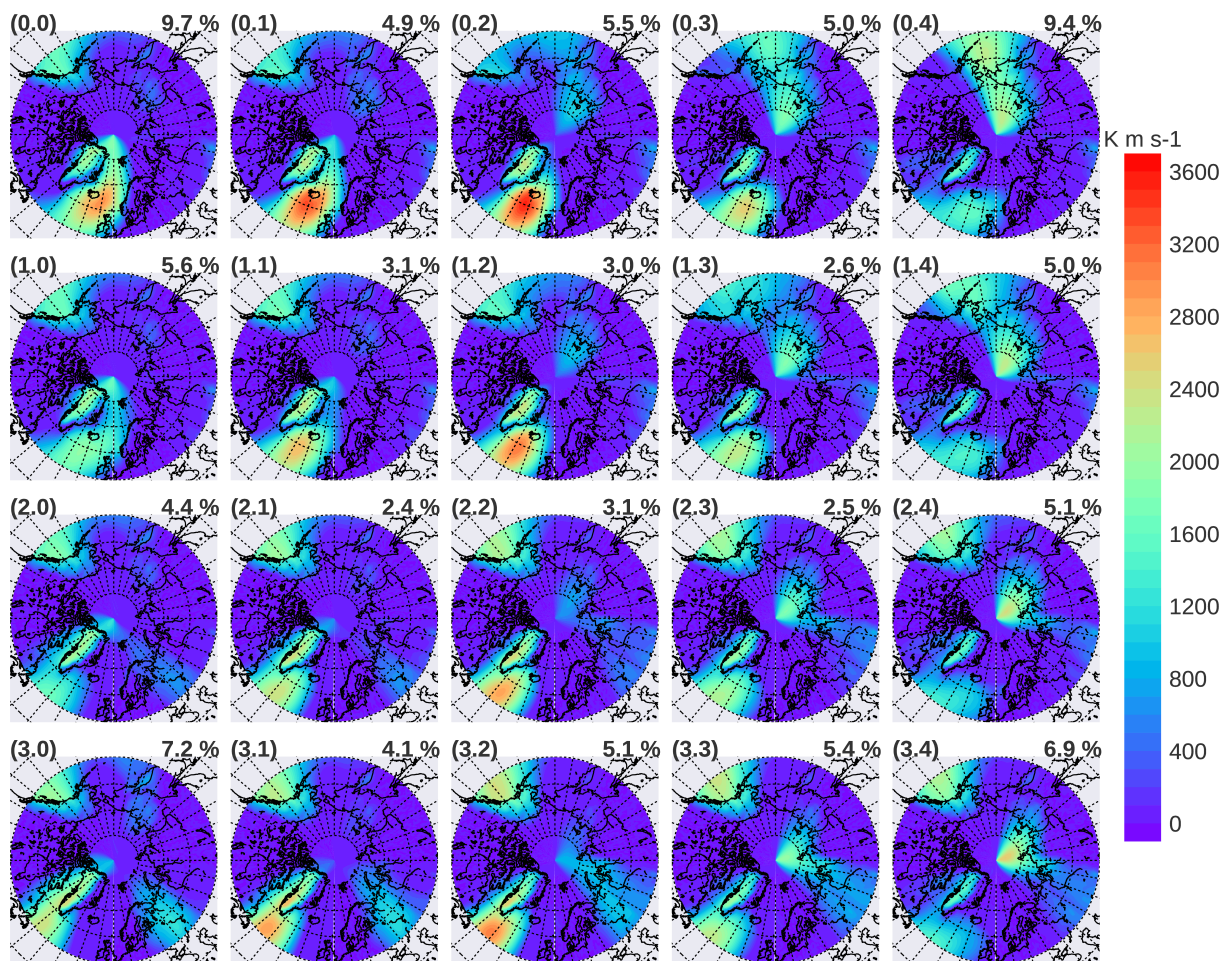
Fig. 1: 4x5 SOM of mean tropospheric (1000 hPa - 200 hPa) meridional temperature flux (vT), of ERA-Interim daily mean data for the winters from 1979/80 to 2015/16; contours show vT in K m s^{-1}, numbers in upper right show occurrence frequency in percent. The numbers in the upper left show the number of the node.

distinguish clusters of pattern within the SOM, which can help to find an appropriate size for the SOM. An appropriate size would consists of enough nodes to find patterns that differ substantially enough without showing too many detailed patterns. Of course, it is dependent on the purpose the SOM has to fulfill: for a very rough generalisation a small SOM is sufficient, for a detailed view on the data a very large SOM is necessary. This is one of the drawbacks of using SOM, the decomposition depends on the chosen size of the map.

Figure 2 shows for each pattern (corresponding to the position within the map) the yearly frequency of occurrence together with a 5 year moving average. For the two patterns of node (0,0), and node (0,4) the time series show the strongest variability. In the year 1990 the conditions similar to the pattern shown in node (0,0) occurs at about 30 % of the winter days, while the pattern of node (0,4) is only present during 2 % of the days in this winter. Looking further into the time series of node (0,0) it can be seen that in 2004 the flux over Iceland has almost never occurred, while the temperature flux through the Bering Strait and the East Siberian Sea is most frequent with 15 %.

The frequency of occurrence of the patterns within the center of the map (nodes (1-2,1-3)) rarely exceeds 10 % and they are present mostly during less 5 % of the days of a year.

The correlation of the time series of the patterns among themselves does not show any specific features (not shown). Only the trends of node (2,0) and node (0,3) show significance with p-values smaller than 0.05. The positive trend of node (2,0) corresponds to relatively low fluxes (about 2000 $\mathrm{K\,m\,s^{-1}}$) through the west coast of Greenland and south of Alaska. Node (0,3) shows a negative trend for slightly higher fluxes (about 2800 $\mathrm{K\,m\,s^{-1}}$) south of Iceland and relatively lower fluxes (about 1600 $\mathrm{K\,m\,s^{-1}}$) through the Bering Strait. Just looking at this node might suggest that states will be less common and other states will increase, but no distinct correlation between the nodes was found.

It has to be noted, that the meridional temperature flux itself could be seen as a representation for the meridional heat flux. No direct influence of this flux on the surface can be derived, for that the divergence of the fluxes have to be analyzed. However, the flux itself is useful to find pathways of transport into the desired regions.

5 Summary and Discussion

An analysis of the patterns of tropospheric mean meridional temperature flux from ERA-Interim reanalysis was performed using an artificial neural network called SOM. With this method it is possible to distinguish key patterns of a given dataset, without the limitation of linear assumptions like in an EOF analysis. Moreover, the SOM can be be analyzed more easily, because the method recreates states that are already present the input data, compared to an EOF were the input data is split up into mathematical orthogonal components. The drawback of this method is that one has to find a reasonable size for the SOM to represent key features without showing to many detailed patterns and thereby loosing generalization.

From the results of our analysis of meridional temperature fluxes it can be suggested that most of the time the meridional heat flux takes place over the North Atlantic between Greenland and Iceland, offshore west Greenland, and through the Bering Strait. These regions are resulting from the geographic features of the northern hemisphere, where the Arctic region is enclosed by land masses and most of the fluxes are channeled over the
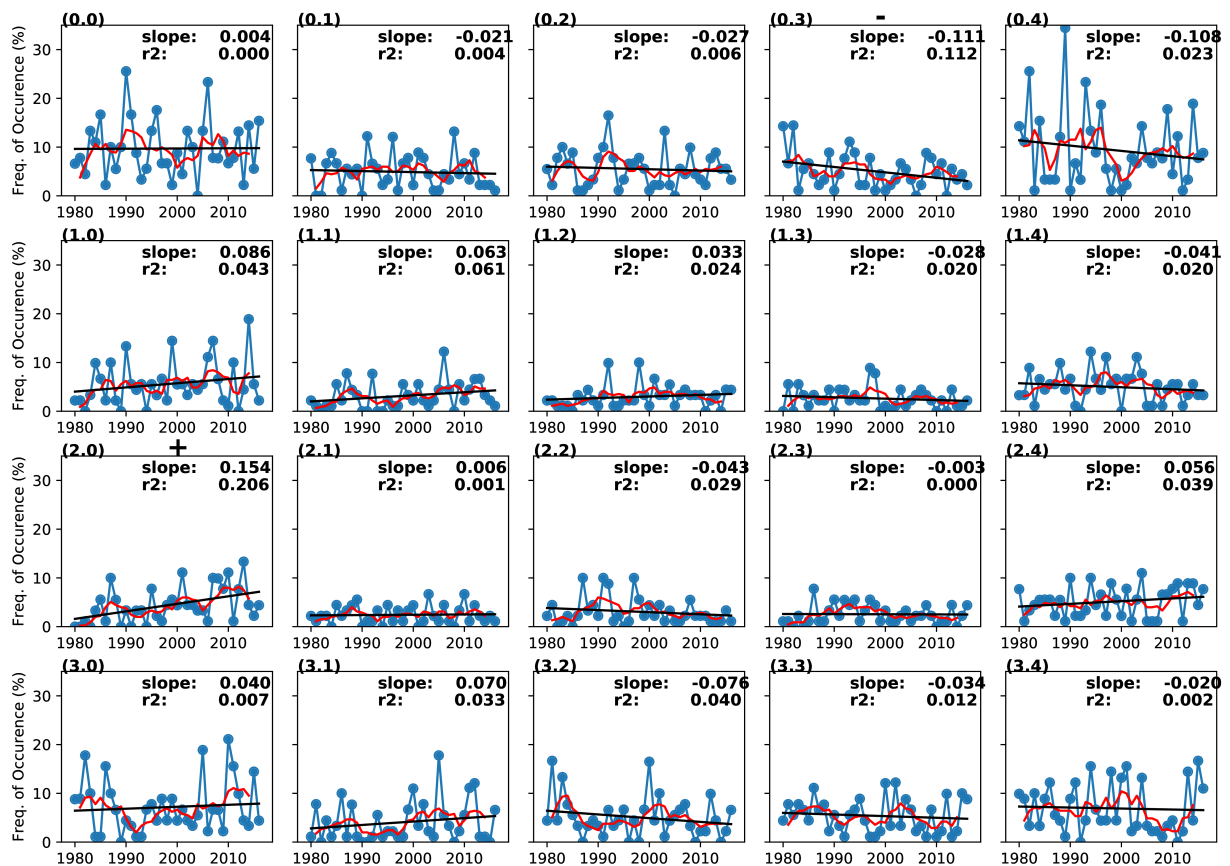
Fig. 2: Time series of the days in each year mapping to the specific state (upper left shows corresponding node/state). Blue lines show percentage of annual days mapping to the specific node, red lines show 5 year moving averages. Black lines show linear fit. In the upper right the slope of the linear fit is shown (in % per year), r^2, the $+$ and $-$ signs at the top of the plots show if the calculated positiv/negative lienar trend is significant or not .

oceans. The time series of the specific patterns show that there are patterns with a large variability and patterns with small variability in the occurrence frequency. The patterns that showed a low frequency of occurrence, which are mostly found in the middle of the map, suggest that the chosen size of the SOM might already be too large to find a more generalized view. Nevertheless, the most frequent pathways that were already found here are consistent with those in the literature (Overland et al., 1996; Adams et al., 2000; Vinogradova, 2007). The strongest fluxes occur over the Denmark Strait and Bering Strait.

Also the pattern looking like wedges of a pie offshore north Siberia might be caused by the choice of daily data. Using daily mean data, synoptic features have to be considered which show these large wedges of temperature flux into the Arctic via Siberia. Those patterns might result from synoptic pressure systems that transport air from northern Siberia into the high-latitude Arctic.

Looking at the frequency of occurrence through time two significant trends were found (see Figure 2). This can be seen by looking at the given p-value which indicates significance above the 95% level for testing the null hypothesis. When this p-value is smaller than 0.05 the trend is considered as significant. In Figure 2 significant trends are indicated by + and − signs depending on the sign of the trend.

Only node (2,0) and node (0,3) contains respectively trend but analysis for different time scales are necessary for further results. This is opposite to the suggestions from Vinogradova (2007), where a negative trend of annual mean meridional heat flux was concluded for January 70°N latitude, which cannot be seen in the trends for the circulation patterns.

For future studies we plan to analyse not only ERA-Interim data but also results from the Coupled Model Intercomparison Project 5 (CMIP5, Taylor et al. (2012)) to see how the models differ from each other and from reanalysis. Further, we will investigate other meteorological variables/fields such as, for example the eddy heat transports and at different time scales, for instance using the method with monthly or yearly mean data. It will also be interesting to look at different patterns of the divergence of heat fluxes. Another possible analysis will be to use the SOM method on 4-dimensional fields (time, level, latitude, longitude) instead of only 3-dimensional fields (time, latitude and longitude) to find patterns/structures that persist within the whole troposphere.

Acknowledgements

References

Adams, J. M., Bond, N. A., and Overland, J. E., 2000: Regional variability of the Arctic heat budget in fall and winter, J. Climate, 13, 3500–3510.

Cassano, E. N., Lynch, A. H., Cassano, J. J., and Koslow, M. R., 2006: Classification of synoptic patterns in the western Arctic associated with extreme events at Barrow, Alaska, USA, Climate Res., 30, 83–97.

Cassano, J. J., Cassano, E. N., Seefeldt, M. W., Gutowski, W. J., and Glisan, J. M., 2016: Synoptic conditions during wintertime temperature extremes in Alaska, J. Geophys. Res. Atmos., 121, 3241–3262.

Cohen, J., Screen, J. A., Furtado, J. C., Barlow, M., Whittleston, D., Coumou, D., Francis, J., Dethloff, K., Entekhabi, D., Overland, J., et al., 2014: Recent Arctic amplification and extreme mid-latitude weather, Nat. Geosci., 7, 627–637.

Colman, R., 2003: A comparison of climate feedbacks in general circulation models, Clim. Dyn., 20, 865–873, doi:10.1007/s00382-003-0310-z.

Dee, D. P., Uppala, S. M., Simmons, A. J., Berrisford, P., Poli, P., Kobayashi, S., Andrae, U., Balmaseda, M. A., Balsamo, G., Bauer, P., Bechtold, P., Beljaars, A. C. M., van de Berg, L., Bidlot, J., Bormann, N., Delsol, C., Dragani, R., Fuentes, M., Geer, A. J., Haimberger, L., Healy, S. B., Hersbach, H., Hólm, E. V., Isaksen, L., Kållberg, P., Köhler, M., Matricardi, M., McNally, A. P., Monge-Sanz, B. M., Morcrette, J.-J., Park, B.-K., Peubey, C., de Rosnay, P., Tavolato, C., Thépaut, J.-N., and Vitart, F., 2011: The ERA-Interim reanalysis: configuration and performance of the data assimilation system, Quart. J. Roy. Meteor. Soc., 137, 553–597, doi:10.1002/qj.828, URL http://dx.doi.org/10.1002/qj.828.

Ford, T. W. and Schoof, J. T., 2017: Characterizing extreme and oppressive heat waves in Illinois, J. Geophys. Res. Atmos., 122, 682–698.

Hewitson, B. and Crane, R., 2002: Self-organizing maps: applications to synoptic climatology, Climate Res., 22, 13–26.

Klocke, D., Quaas, J., and Stevens, B., 2013: Assessment of different metrics for physical climate feedbacks, Clim. Dyn., 41, 1173–1185, doi:10.1007/s00382-013-1757-1.

Kohonen, T., 1998: The self-organizing map, Neurocomputing, 21, 1–6.

Liu, Y. and Weisberg, R. H., 2011: A review of Self-Organizing Map Applications in Meteorology and Oceanography, Dr Josphat Igadwa Mwasiagi, doi:10.5772/13146.

Lynch, A. H., Serreze, M. C., Cassano, E. N., Crawford, A. D. and Stroeve, J., 2016: Linkages between Arctic summer circulation regimes and regional sea ice anomalies, J. Geophys. Res. Atmos., 121, 7868–7880.

Mattingly, K. S., Ramseyer, C. A., Rosen, J. J., Mote, T. L. and Muthyala, R., 2016: Increasing water vapor transport to the Greenland Ice Sheet revealed using self-organizing maps, Geophys. Res. Lett., 43, 9250–9258.

McDonald, A. J., Cassano, J. J., Jolly, B., Parsons, S. and Schuddeboom, A., 2016: An automated satellite cloud classification scheme using self-organizing maps: Alternative ISCCP weather states, J. Geophys. Res. Atmos., 121.

Overland, J. E., Turet, P. and Oort, A. H., 1996: Regional variations of moist static energy flux into the Arctic, J. Climate, 9, 54–65.

Reusch, D. B., Alley, R. B. and Hewitson, B. C., 2005: Relative Performance of Self-Organizing Maps and Principal Component Analysis in Pattern Extraction from Synthetic Climatological Data, Polar Geo., 29, 188–212, doi:10.1080/789610199.

Stroeve, J. C., Serreze, M. C., Holland, M. M., Kay, J. E., Malanik, J. and Barrett, A. P., 2012: The Arctic's rapidly shrinking sea ice cover: a research synthesis, Climatic Change, 110, 1005–1027.

Taylor, K. E., Stouffer, R. J. and Meehl, G. A., 2012: An overview of CMIP5 and the experiment design, B. Am. Meteorol. Soc., 93, 485–498.

Vinogradova, A., 2007: Meridional mass and energy fluxes in the vicinity of the Arctic border, Izv. Atmos. Ocean Phys., 43, 281–293.

Wendisch, M., Brückner, M., Burrows, J., Crewell, S., Dethloff, K., Ebell, K., Lüpkes, C., Macke, A., Notholt, J., Quaas, J., et al., 2017: Understanding Causes and Effects of Rapid Warming in the Arctic, EOS, 98.

Wittek, P., 2013: Somoclu: An Efficient Distributed Library for Self-Organizing Maps, CoRR, abs/1305.1422.